3D BRAIN STRUCTURES EXTRACTION USING FULLY AUTOMATED MRI SEGMENTATION

Laurent VERARD (1)(2), Pascal ALLAIN (2), Jean-Marcel Travere (2)(3), Su RUAN (4), Daniel BLOYET (4)

(1) URA 1829 CNRS - (2) GIP CYCERON, Bd Becquerel, BP 5229, 14074 Caen Cedex, France
(3) CEA/DSV/DRIPP - (4) GREYC - URA 1526 CNRS, Bd Maréchal Juin, 14050 Caen, France

RESUME

Les progrès en techniques d'imagerie médicale et du matériel informatique ont donné beaucoup d'importance à la troisième dimension dans des domaines variés tels que le pronostic, le diagnostic ou pour les corrélations anatomico-fonctionnelles ou chirurgicales pour le cerveau. Beaucoup de méthodes de segmentation du cerveau humain à partir d'Images par Résonance Magnétique (IRM) offrent uniquement un résultat d'extraction de l'encéphale avec souvent une intervention manuelle. Le but de cet article consiste à montrer une segmentation entièrement automatique de l'encéphale mais aussi du cerveau sans cervelet ni tronc cérébral et la séparation des deux hémisphères.

ABSTRACT

Progress in imaging modalities and graphic workstations have rendered important the third dimension in various fields such the anatomofunctional correlations in the brain where both prognostic and diagnostic applications are possible. Many segmentation methods for the magnetic resonance images (MRI) of the human brain extract the whole organ though usually manual intervention is required. We here demonstrate that it is not only possible to segment the entire brain by a fully automated process but also to separate the cerebral hemispheres from the brain stem and the cerebellum.

I. INTRODUCTION

By 3D Magnetic Resonance Imaging (MRI), brain anatomy can now be investigated at high resolution, using procedures referred to as "segmentation". One of the current challenges is to establish fully automated and individual techniques with high robustness for segmentation of MRI data and final three-dimensionnal (3D) visualisation [1]. There are mainly two approaches in segmentation. The first one is based on transitions or boundary detection between homogeneous zones using a derivation operators principle. This "Contour" approach has already been applied to brain MRI data in the 3D [2] case, in order to optimize tissue border locations. However, this approach is limited by the large number of contours with respect to the signal noise ratio (SNR) and by problems due to unclosed contours. The second approach consists of searching homogeneous zones whose pixels share one or several properties with a connectivity algorithm [3][4]. Breaking undesired connections on 2D images with morphological operators [5] presents drawbacks of the correction of the 2D results by using an overlap procedure to propagate the information in the third dimension or the need of human intervention. Other difficulties are due to some connections which are true anatomical links while some others are artifacts due to a partial volume effect. The present study, inspired by the above cited works, establishes a fully automated method for 3D encephalon, brain or hemisphere MRI segmentation.

II. METHOD

The flowchart of the fully automated 3D brain MRI segmentation method is presented in Fig. 1.

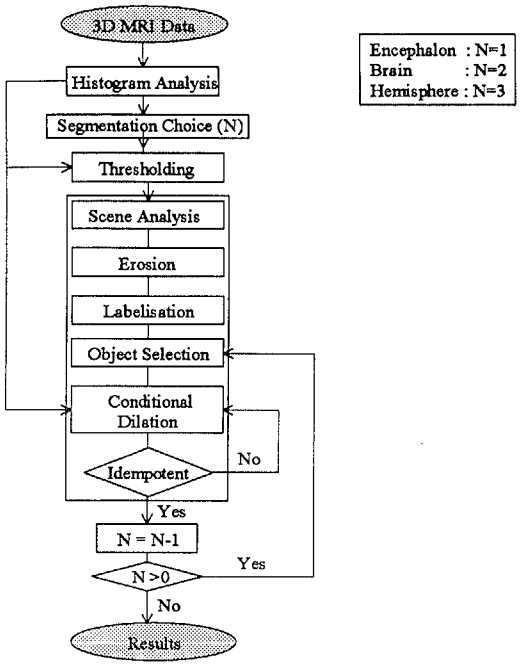

Figure 1 : General Flowchart of the segmentation method.

The pre-processing step consists of a grey scale histogram analysis which allows automatic thresholds selection for the scene analysis and the conditional dilatation. After a grey scale thresholding, which also reduces parasitic connections with the surrounding structures either of low (e.g. skull) or high (e.g. eye orbits) grey level, a scene analysis in the inter-hemispheric plan is used in cases of brain or hemisphere segmentation to cut automatically true anatomical links. Then, a binary erosion, using a 3D structuring element which only takes the six first neighbours into account, is applied twice in order to insure the breaking of some parasitic links. During the labelling process, if the segmentation choice is N, the largest N objects are preserved . Then, the region to be segmented is selected automatically [6]. Thus, the conditional dilatation recaptures the lost voxels during the erosion, through the use of grey scales given by the calculated histogram and a 3D connectivity algorithm, until no new voxel is added to the seed. As soon as N=0, the process stops and gives the result.

The process automation is due to a robust analysis of the grey scale histogram. It permits to select thresholds for a scene analysis or an erosion procedure. To establish the initial threshold, the histogram is calculated in a sub volume SV in order to recognize the cerebrospinal fluid (CSF), the white matter (WM) and grey matter (GM).

With the sequence used and in the absence of contrast medium in patients who do not present with a pathology which itself alters the observed grey level scaling, the histogram always shows a specificity for levels associated to WM and GM. Based on the analysis of alarge number of MRI data sets obtained according to our specific acquisition parameters and for a scene analysis on a binary image in the inter hemispheric plane, the suitable initial grey level threshold is T_l. For the segmentation procedure, two grey scale bands are defined based on three grey scale values Th, Tl and Tl' given by : $\sum_{i=Ival}^{Th} pi \,/\, \sum_{i=Ival}^{IMAX} pi \approx 0.85$

where p_i is the population of the grey level i, I_{MAX}=255 and I_{val}=grey level of the valley between background and CSF.

$$\sum_{i=Ival}^{Tl} pi \,/\, \sum_{i=Ival}^{IMAX} pi \approx 0.45 \text{ and } \sum_{i=Ival}^{Tl'} pi \,/\, \sum_{i=Ival}^{IMAX} pi \approx 0.20 .$$

Since the erosion altered several regions, it is important to recover some of them with a dilatation algorithm which takes brain morphology into account, starting from the seed and growing up according to connectivity restrictions and grey scales bands. This conditional dilatation is separated into two consecutive steps, the first one (D_1) operating on the upper band within the range [Tl ; Th] and the second one (D_2) operating on the lower band within the range [Tl' ; Th]. D1 allows to recover the object framework and to recapture the lost voxels during erosion steps without recapturing parasitic bridges ; the process does not stop until no new voxel is added to the set of connected voxels or, when the number of added voxels increases again (which corresponds to a parasitic connection). During D2, this core obtained with D_1 will be used as the seed which will grow up by recovering the GM voxels close to the CSF. Once again, this process does not stop until no new voxel is added to the set of connected voxels or when the number of added voxels increases

again (which corresponds to a parasitic connection). Each dilatation D_i takes brain morphology into account, whether it is ramified or not, with a spatial investigation of voxels on two consecutive layers. Let x, be a voxel, still set to 0, on the peripheral layer exterior to the seed. We test if x will join, or not, the seed by taking its neighbours into account. During D_i process, four conditions, given by the numbers m_i, n_i, p_i, q_i of the voxel x neighbourhood, must be accepted to perform the fact that x joins the seed. D_1 is performed on a seed set to 1. We first test m_1, the number of the neighbours of the voxel x on this layer in a 3x3x3 voxels surrounding zone within the grey scale range [Tl ; Th] ; x is able to join the seed if at least m_1 neighbours answer the purpose. The second parameter, n_1, is the number of the neighbours of the voxel x on the same layer in a 5x5x5 voxels surrounding zone ; it is tested within the same grey scale range ; x is able to join the seed if at least n_1 neighbours serve the purpose. For the other two parameters, p_1 and q_1, following the same way, the neighbourhood of x is tested on the peripheral layer interior to the seed in order to insure a continuity of the object between the layers L_k and L_{k+1}. If at least p_1 neighbours (set ot 1) of the voxel x in a 3x3x3 voxels surrounding zone and q_1 neighbours (set ot 1) of the voxel x in a 5x5x5 voxels surrounding zone answer the purpose, x is able to join the seed. D_2 is then applied on the "new" seed obtained after D1 within the grey scale range [Tl' ; Tl] taking the other four parameters m_2, n_2, p_2, q_2 into account. If the four conditions are respected, the voxel x joins the seed otherwise waits for a further moment in the loop to be joined.

III. RESULTS AND DISCUSSION

The method described above has been exploited not only for the encephalon segmentation but also for brain or hemisphere segmentation (see Figure below).

This procedure was designed to operate on MRI scans, which offer a good contrast between each structure

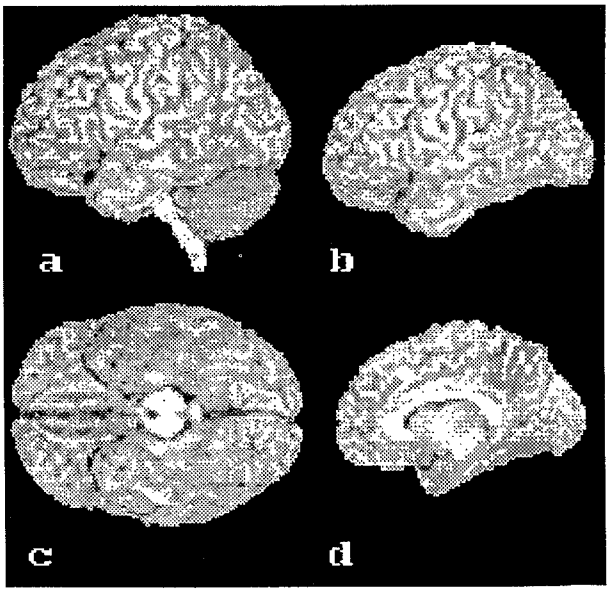

Results : (a) encephalon (b) brain (c) basal view of the brain without brain stem and cerebellum (d) right hemisphere.

of interest and the surrounding structures. The resulting T_1-weighted scan protocol, further constrained by clinical scan time limitations, has the following parameters : volume = 256x256x124, sagittal orientation which limits flow artifacts, SPGR sequence with a flip equal to 35°, field of view (FOV) = 33 cm, voxel volume = 1.3^3 mm^3, contiguous 1.3 mm thick slices, TR = 24 ms, TE = 9 ms, 9.5 min acquisition time on General Electric Signa Advantage 1.5T of the University Hospital of Caen. Our software was performed on a Silicon Graphics Indigo Workstation.

Up to now, for a set a 20 normal patients considered, the process applied never failed. Parameters m,n,p,q are adjusted to the morphology of the cerebellum (CB) and the brain. Our method is applied on the structure to be segmented according to a priori knowledges : to segment the brain without CB and the brain stem (BS), an automated cut of BS is needed thanks to a scene analysis in the mid-sagittal plane [6][7]. The method is well adapted for 3D automated segmentation. Usually, other solutions need a manual intervention. The accuracy of the brain segmentation is ultimately limited by the quality of the data and the pathology of the patient. The originality of this work is the 3D visualization of the basal and mid-sagittal sulci. Our

histogram analysis has permitted the automatic selection of threshold values, which never alter our segmentation. The advantage of our method allows an automated detection of gyri on lateral [8], inferior or in inter-hemispheric faces. These segmentations are useful for a registration on Positron Emission Tomography (PET) scans [9] and also as an a priori information in PET reconstruction algorithms. It is also a helpful tool for the pathologist since he can see for example an infarct on the anatomical surface.

This work has been performed under the auspices of the "Centre Pôle Traitement et Analyse d'Images"-"Image Processing Centre".

REFERENCES

[1] M. Bomans, K.H. Höhne, G. Laub, A. Pommert, U. Tiede, "Improvement of 3D acquisition and vizualisation in MRI", Magn.Res.Imag., vol. 9, pp. 597-609, 1991.

[2] M. Bomans, K. H. Höhne, U. Tiede, M. Riemer, "3D segmentation of MR images of the head for 3D display", IEEE Trans. Med. Imag., vol. 9, pp. 177-183, June 1990.

[3] H. E. Cline, C. L. Dumoulin, H. R. Hart, Jr., W. E. Lorensen and S. Ludke, "3D reconstruction of the brain from magnetic resonance images using a connectivity algorithm", Magn. Res. Imag., vol. 5, pp. 345-352, 1987.

[4] M. E. Brummer, R. M. Mersereau, R. L. Eisner and R. R. J. Lewine, "Automatic detection of brain contours in MRI data sets", IEEE Trans. Med. Imag., vol. 12, No. 2, pp. 153-166, June 1993.

[5] K. H. Höhne and W. A. Hanson, "Interactive 3D segmentation of MRI and CT volumes using morphological operations", Journ. Comp. Assist. Tomog., vol. 16, No. 2, pp. 285-294, Mar./Apr. 1992.

[6] J. Talairach, G. Szikla, P. Tournoux, A. Prossalentis, M. Bordas-Ferrer, L. Covello, M. Jacob, E. Mempel, "Atlas d'anatomie stéréotaxique du télencéphale : études anatomo-radiologiques", Ed. Masson & Cie, Paris, 1967.

[7] H. M. Duvernoy, E. A. Cabanis, M. T. Iba-Zizen, J. Tamraz and J. Guyot, "Le cerveau Humain", Springer-Verlag France, Paris, 1992.

[8] M. Desvignes, H. Fawal, M. Revenu, D. Bloyet, J.M. Travere, P. Allain, J.C. Baron, "Reconnaissance du sillon latéral du cortex sur des images tridimensionnelles", Congrès AFCET RFIA, Paris, pp. 685-690, 1994.

[9] P. Allain, J.M. Travere and al., "Accurate PET positionning with reference to MRI and neuroanatomical data bases", in Brain PET '93 Akita Proceedings, Akita, Japan, pp. 401-408, May 1993.